Journal of Environmental Management 353 (2024) 120113

Contents lists available at ScienceDirect

Journal of Environmental Management

journal homepage: www.elsevier.com/locate/jenvman

Research article

Contributions of climate change and urbanization to urban flood hazard changes in China's 293 major cities since 1980

Ziyi Tang [a], Pin Wang [a,b,*], Yao Li [c], Yue Sheng [a], Ben Wang [a], Nataliia Popovych [d], Tangao Hu [a,b]

[a] Institute of Remote Sensing and Earth Sciences, Hangzhou Normal University, Hangzhou, 311121, China
[b] Zhejiang Provincial Key Laboratory of Urban Wetlands and Regional Change, Hangzhou, 311121, China
[c] Faculty of Geo-Information Science and Earth Observation (ITC), University of Twente, AE, Enschede, 7500, Netherlands
[d] School of Geology, Geography, Recreation and Tourism, V. N. Karazin Kharkiv National University, Kharkiv, 61022, Ukraine

ARTICLE INFO

Handling Editor: Jason Michael Evans

Keywords:
Climate change
Urbanization
Urban flood hazard
Surface runoff
China

ABSTRACT

The growing incidence of urban flood disasters poses a major challenge to urban sustainability in China. Previous studies have reported that climate change and urbanization exacerbate urban flood risk in some major cities of China. However, few assessments have quantified the contributions of these two factors to urban flood changes in recent decades at the nationwide scale. Here, surface runoff caused by precipitation extremes was used as the urban flood hazard to evaluate the impacts of climate change and urbanization in China's 293 major cities. This study assessed the contributions of these drivers to urban flood hazard changes and identified the hotspot cities with increased trends under both factors during the past four decades (1980–2019). The results showed that approximately 70% of the cities analyzed have seen an increase of urban flood hazard in the latest decade. Urbanization made a positive contribution to increased urban flood hazards in more than 90% of the cities. The contribution direction of climate change showed significant variations across China. Overall, the absolute contribution rate of climate change far outweighed that of urbanization. In half of the cities (mainly distributed in eastern China), both climate change and urbanization led to increased urban flood hazard over the past decade. Among them, 33 cities have suffered a consecutive increase in urban flood hazard driven by both factors.

1. Introduction

Urban flood disaster is globally recognized as one of the most hazardous and frequent disasters, causing extensive damage to city infrastructure and society (Blöschl et al., 2019; Tellman et al., 2021). For example, the flood event in Shenzhen on April 11, 2019 led to 11 fatalities in Chegongmiao metro station (Lyu et al., 2020). The devastating flood event in Zhengzhou on July 20, 2021 caused approximately 380 deaths and missing cases, along with a staggering direct economic loss of over \$5.7 billion (Disaster Investigation Team of State Council, 2022). Due to the dense population and extensive urban infrastructure, urban flood disasters are increasingly posing a challenge to the sustainable development of China (Liu et al., 2022; Yang et al., 2023). Therefore, understanding the spatio-temporal patterns of urban flood change and identifying the hotspot cities in China's major cities over the past decades, can provide perspectives for nationwide policymakers for the effective management of urban flooding risks in a changing environment.

Based on the disaster records from China Yearbook (2001–2020), Li and Zhao (2022) found that direct economic losses caused by floods have increased across China. Based on the disaster census data of rainstorm-induced flood in 637 counties in East China, the study of Shi et al. (2020) indicated that the number of records of flood disaster increased at a rate of 77.4 times per decade from 1984 to 2010. Particularly, in eight Chinese megacities (Beijing, Guangzhou, Nanjing, Shanghai, Shenzhen, Tianjin, Wuhan and Xian), Li et al. (2022) used the urban flood records from 2015 to 2020 and analyzed the distribution of urban flood points in different cities. This study indicated that the occurrence of urban flood events showed quite different patterns across China. However, owing to data limitations in the long time series of urban flood records, the temporal trend was not examined in previous work. Previous studies typically utilized urban precipitation as an indicator to examine the temporal trend of urban flood hazards. For example, Liang et al. (2019) studied urban precipitation characteristics in 2264 Chinese cities, and revealed that the majority of cities have experienced an upward trend in extreme precipitation. However, the

* Corresponding author. Institute of Remote Sensing and Earth Sciences, Hangzhou Normal University, Hangzhou, 311121, China.
E-mail address: wangpin@hznu.edu.cn (P. Wang).

https://doi.org/10.1016/j.jenvman.2024.120113
Received 5 October 2023; Received in revised form 9 January 2024; Accepted 12 January 2024

surface runoff caused by precipitation extremes should better describe the hazard rather than the intensity of extreme precipitation alone (Beshir and Song, 2021; Wang et al., 2023). Using this indicator should help improve the understanding of the spatio–temporal patterns of urban flood changes across China.

Furthermore, understanding the drivers behind changing flood risks is essential to identify urban flooding hotspots and indicate adaptation measures. Precipitation extremes have changed under continued global climate changes. In Liang et al.'s study (2019), extreme precipitation in most cities has upward trends. This could increase stormwater runoff, urban drainage and finally led to more urban flood events (Sun et al., 2021; Zhou et al., 2018, 2019). Projections for 2030 suggest that a growing proportion of the population will face increased exposure to floods due to climate change (Tellman et al., 2021). Since China's 1978 "Reform and Opening-up", most cities in China have experienced accelerated urbanization. When the intensity of rainfall surpasses the infiltration capacity, cities with larger areas of impervious surfaces are more prone to flooding, even under the same amount of precipitation. Based on high-resolution annual data, the study of Rentschler et al. (2023) illustrated that human settlements worldwide have continuously and rapidly encroached upon current food zones since 1985. Overall, climate change and urbanization are two of the most influential drivers that pose challenges to current and future urban flood management strategies (Chen et al., 2021; Jiang et al., 2023; Wang et al., 2023).

Several studies have been conducted to evaluate the impacts of climate change or urbanization. In terms of climate change impact, previous studies have generally kept land use data and other inputs fixed, while only modifying rainfall intensities between two periods (Hou et al., 2022; Wang et al., 2023; Zhou et al., 2018). For example, in the study of Hou et al. (2022), they used a hydrodynamic inundation model to evaluate the impact of future climate change on flooding duration and maximum inundation area in the Future Science City Park in Beijing, China. This study utilized the latest available land use data, and examined rainfall intensities during three time periods: the baseline (1976–2005), near-future (2020–2049), and long-term-future (2060–2089) periods. It was found that the total flooding volume is projected to increase by 171%–716% under 20-year rainfall events in the two future periods, compared to the baseline level. Regarding the impact of urbanization, previous studies generally maintained fixed precipitation data and other inputs while only modifying the land use data (Beshir and Song, 2021; Luo and Zhang, 2022; Zhou et al., 2019). For instance, in the study of Luo and Zhang (2022), they used the Soil and Water Assessment Tool to evaluate the impact of land use/cover change (LUCC) caused by urbanization on urban flood regulation service in China's major cities. In this study, the same rainfall scenario was applied, and land-use data from both 1977 and 2018 were utilized. It was revealed that LUCC has caused a 13.39% decline in China's urban flood regulation service from 1977 to 2018. In summary, the prevailing approach of isolating the impacts of climate change or urbanization involves recalculating urban flood changes while holding one factor constant. However, previous studies have often focused solely on a single type of impact (either climate change or urbanization). Since different indices and study periods were used in these studies, it is difficult to make direct comparisons between the impacts of these two factors in major cities across China. Therefore, conducting comprehensive nationwide quantitative assessments using a consistent framework is critical to determining how climate change and urbanization have affected changes in urban flood hazards over recent decades. This will significantly contribute to the development of effective adaptation strategies and greatly enhance the resilience of cities across China.

To fill the gap in large-scale analysis, this study used the soil conservation service curve number (SCS–CN) model to calculate surface runoff and assess urban flood hazards. The present study utilized the precipitation data from 2472 meteorological observation stations in addition to land use, soil, and digital elevation model (DEM) data during the past four decades (1980–2019). The hazard analysis was further decomposed to evaluate the contributions of urbanization and climate drivers to urban flood hazard changes. Accordingly, this study identified the hotspot cities with a consecutive increase under the impacts of both two factors across China's 293 major cities. These findings are crucial to inform future mitigation and adaptation strategies under non-stationary conditions.

2. Materials and methods

2.1. Study area and data sources

Based on the latest version of the administrative divisions published by the Ministry of Civil Affairs of the People's Republic of China, there are 293 prefecture-level cities in China (Fig. 1). The study area does not include Hong Kong, Macau, or Taiwan Province. It is divided into eight regions based on the terrain and economic conditions. The specific names of all the cities included are presented in Fig. S1 and Table S1. The vector boundaries and maps published by the Information Centre of the Ministry of Natural Resources of China were obtained, and an urban polygon map was used to display the administrative divisions of all cities. In this study, the main (or core) urban area was used to represent the urban scope of each city. In eastern China, the urban scope is generally small. Using a polygon map could not clearly show the values of these cities. Following the approach in Peng et al.'s study (2022), the polygon map is also provided in the Supplementary Material (Fig. S1), while the other spatial maps are point maps.

China's reform and opening-up policy began in 1978, and since then, the number of cities has undergone a rapid development stage (Cao and Zhang, 2022; Zhang and Li, 2021): From 1978 to 2003, the total number of prefecture-level cities in China increased from 98 to 282; And a total of 267 adjustments were made to China's prefecture-level administrative divisions; Since 2003, the number of cities has remained relatively stable, with minor adjustments still occurring in zoning. Considering this situation, it is difficult to track the changes in the administrative divisions of the 293 prefecture-level cities examined in this study. Therefore, we used the latest vector of administrative division in 2019 to encompass the widest range of urban areas from 1980 to 2019. By keeping this vector fixed, it is possible to eliminate the impact of city boundary changes caused by policy factors. This approach has also be used in the previous studies (e.g., Luo and Zhang, 2022; Peng et al., 2022). Urban flood disasters often occur in the core areas of cities. As a result, our research focused solely on urban growth within the core areas of each city, without considering the expansion of city boundaries. We calculated urban growth by examining changes in the proportion of urban built-up area in the core areas of each city. The urbanization index is reflected comprehensively in the changes of land use type, primarily through the transformation from non-built-up areas to urban built-up areas.

In this study, datasets of China's DEM, soil type, and land-use type with a resolution of 1 km × 1 km were obtained from the Resource and Environment Science and Data Center (RESDC) of the Chinese Academy of Sciences. As described by the RESDC, the land-use type data were obtained by manual visual interpretation based on Landsat images. This nationwide land-use database produced by using high-resolution satellite remote-sensing images, has been extensively validated for its accuracy throughout China (Liu et al., 2014). Moreover, it has been widely utilized in numerous studies (e.g., Chen et al., 2021; Wang et al., 2019; Zhang et al., 2020), which validates its suitability for our research. Because there was little change in soil type and DEM data during the historical period, only one map of soil type/DEM could be obtained from the RESDC. The observed records of daily precipitation (1980–2020) were collected from the China Meteorological Administration. In total, 2472 meteorological stations were used in this study, which could fully cover the study area.

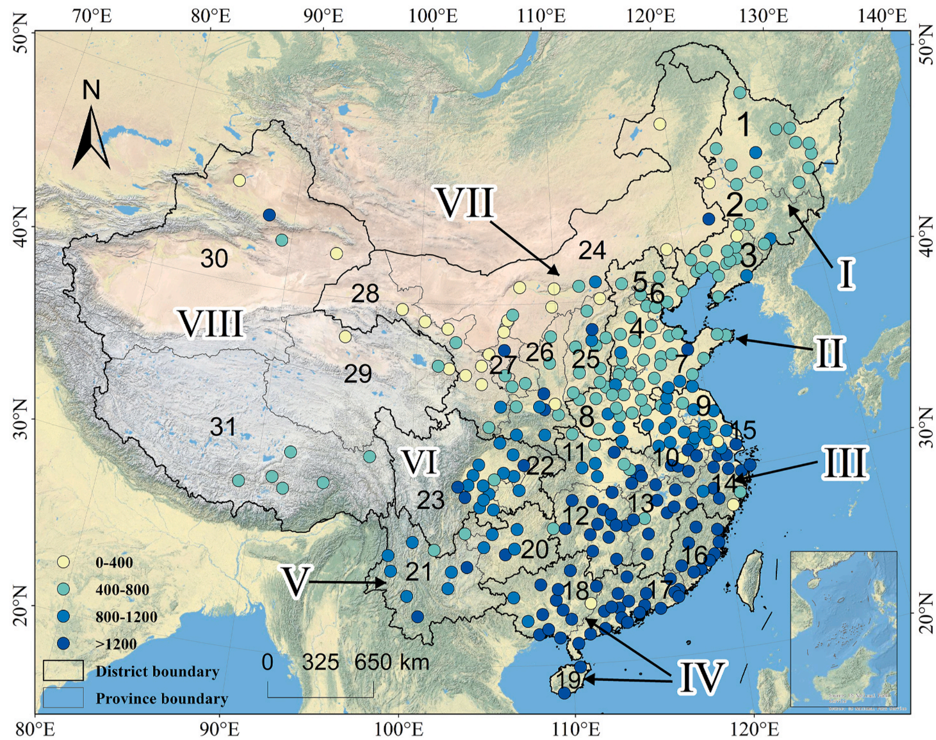

Fig. 1. Locations and average annual precipitation (mm) of 293 prefecture-level cities in China. Region I–Northeast China (including 1 Heilongjiang, 2 Jilin, and 3 Liaoning); Region II–the North China Plain (including 4 Hebei, 5 Beijing, 6 Tianjin, 7 Shandong, and 8 Henan); Region III–the mid-lower reaches of the Yangtze River (including 9 Jiangsu, 10 Anhui, 11 Hubei, 12 Hunan, 13 Jiangxi, 14 Zhejiang and 15 Shanghai); Region IV–South China (including 16 Fujian, 17 Guangdong, 18 Guangxi, and 19 Hainan); Region V–the Yunnan-Guizhou Plateau (including 20 Guizhou and 21 Yunnan); Region VI–the Sichuan Basin (including 22 Chongqing and 23 Sichuan); Region VII–the Loess Plateau (including 24 Inner Mongolia, 25 Shanxi, 26 Shaanxi, 27 Ningxia and 28 Gansu); Region VIII–West China (including 29 Qinghai, 30 Xinjiang and 31 Tibet).

2.2. Assessment of urban flood hazard

In accordance with previous studies (Beshir and Song, 2021; Hu et al., 2020), the surface runoff caused by extreme precipitation events was used to quantify urban flood hazards. The SCS-CN method is a popular technique for calculating surface runoff (Mishra and Singh, 2003; Verma et al., 2021; Yin et al., 2017). It has been confirmed to be highly effective in capturing the temporal trend of urban runoff in some major cities (Li et al., 2018; Mahmoud and Gan, 2018; Wang et al., 2023). The calculation of surface runoff can be described in brief as follows.

In the SCS-CN method, the runoff volume is determined by the precipitation extreme, initial abstraction, and hydrologic storage using Eq. (1). The major equations used are as follows:

$$R = \begin{cases} \dfrac{(P-\lambda \bullet S)^2}{P+(1\text{-}\lambda) \bullet S} & P > \lambda \bullet S \\ 0 & P \leq \lambda \bullet S \end{cases} \quad (1)$$

where R indicates the surface runoff (mm) caused by the precipitation event; P is the intensity of the precipitation extreme (mm, $P \geq R$); S indicates the potential maximum retention (mm); and λ is the initial abstraction ratio (dimensionless).

In this study, the average daily precipitation >99th quantile (P99) was used to represent the average level of extreme precipitation events that occurred in a city. The P99 value index is often used to depict critical precipitation (Xu et al., 2022). Generally, precipitation extremes can show large inter-annual variation. In this study, the P99 index in each decade was calculated, and the inter-decadal trend was assessed. This study divided 1980–2019 into four decades: the 1980s, 1990s, 2000s, and 2010s. In each decade, the P99 value was calculated based on the data from meteorological stations. These values were then interpreted for each 1 km × 1 km grid based on nearest-neighbor interpolation. The nearest-neighbor interpolation approach has proven to be useful and effective when data are evenly spaced in China (Chen et al., 2021; Peng et al., 2019; Wang et al., 2023). As there are more than 2400 stations relatively evenly distributed across the study area, the nearest-neighbor interpolation method was used in this study.

In Eq. (1), λ is originally set as 0.20, which is suited to zones with slopes no more than 5.00%. In order to depict various the topographic conditions across China, λ should be adjusted with slope (Pang et al., 2020; Wang et al., 2023). The slope adjustment factor for λ is calculated as follows.

$$f(slope) = e^{-0.083 \bullet slope} \quad (2)$$

where the unit of *slope* is degree (°).

In Eq. (1), the potential maximum retention (S) is calculated by Eq. (3):

$$S = \frac{25400}{CN} - 254 \quad (3)$$

CN depends on the antecedent soil moisture condition (AMC), soil type and land cover type. Generally, AMC could be divided into three classes: I (dry), II (average) and III (wet) (U. S. Soil Conservation Service, 1972). Inconsistent with Wang et al. (2023), we calculated average annual precipitation (P_{avg}) during the study period to define AMC level: $P_{avg} < 400$ mm for AMCI, 400 mm $\leq P_{avg} < 800$ mm for AMCII, and $P_{avg} \geq 800$ mm for AMCIII.

By using Eqs. (4) and (5) (Neitsch et al., 2011), CN for AMCI and III could be calculated.

$$CN_1 = CN_2 - \frac{20 \bullet (100 - CN_2)}{(100 - CN_2 + exp[2.533 - 0.0636 \bullet (100 - CN_2)])} \quad (4)$$

$$CN_3 = CN_2 \bullet exp[0.00673 \bullet (100 - CN_2)] \tag{5}$$

where CN_1 CN_2 *and* CN_3 indicate CN for AMCI, II and III, respectively.

In this study, we calculated *CN* for AMCII based on Tables 1 and 2. Besides, we used the slope adjusted method for CN proposed by Huang et al. (2006). The calculation method is as follows.

$$CN_{sl} = CN \bullet \left(\frac{15.63 \bullet slope + 322.79}{slope + 323.52} \right) \tag{6}$$

where the unit of *slope* is m m^{-1}.

In our previous study (Wang et al., 2023), the reliability of simulated surface runoff has been verified by the comparison with the China Natural Runoff Dataset version 1.0 (Miao et al., 2022; Gou et al., 2020, 2021). The absolute errors between the calculated levels of surface runoff and actual measurements during 1995–2014, range from 40 mm to 90 mm. And the relative errors are between 5% and 16%. This indicated that these runoff simulations could well describe the actual measurements in China.

2.3. Analysis

(1) Assessing the inter-decadal trend of urban flood hazard and its driving factors

The level over the 1980s was used as the baseline level. The changes over the 1990s, 2000s, and 2010s relative to the baseline level were calculated. To fully depict the inter-decadal trends of urban flood hazard and its driving factors, six types of temporal trend patterns were used based on the levels over the 1990s, 2000s, and 2010s (Table 3). Specifically, the changes could be divided into two main types based on the change over the past two decades. If an increase was found from the 2000s–2010s, the trend type was defined as Type I. Type I trends could be divided into three subtypes, as shown in Table 3. Type I2 was the pattern of a continuous increase during the 1990s–2010s. If a decrease was found from the 2000s–2010s, the trend was considered Type D. Type D2 trends exhibited a continuous decrease during the 1990s–2010s.

In this study, the index of urban growth rate calculated by examining changes in the proportion of urban built-up area in the core region of each city (shown in Fig. S1), is used to briefly reflect the urbanization extent. The equation is as follows.

$$UG = \frac{PUB_{t_2} - PUB_{t_1}}{PUB_{t_1}} \times 100\% \tag{7}$$

where *UG* (%) indicates the urban growth rate; PUB_{t_1} and PUB_{t_2} are the proportions of the number of urban built-up grids to the total number of grids in the core region of each city in the t_1 and t_2 periods, respectively. Here, urban built-up grids included the types of "high-density urban land" and "low-density urban land" from the land-use database.

Table 1
CN values based on land use and soil type.

Land use	Soil groups of hydrology			
	A	B	C	D
High-density urban land	90	93	94	95
Low-density urban land	60	74	83	87
Cultivated land	67	78	85	89
Forest land	25	55	70	77
alvar	36	60	74	80
orchard	40	62	76	82
wetland	32	58	72	79
Bare land	72	82	88	90
water	98	98	98	98

Table 2
Soil types and hydrological properties.

Soil type	Soil hydrological properties
A	Thick sand, thick loess, granulated silty sand
B	Thin layer loess, sandy loam
C	Clay loam, thin sandy loam, soil with low organic matter content, soil with high clay content
D	Soil that expands significantly after absorbing water, plastic clay, certain saline soils

Table 3
Six types of the trend patterns.

Type	Subtype 1	Subtype 2	Subtype 3
D Decrease from the 2000s–2010s	D1 	D2 	D3 
I Increase from the 2000s–2010s	I1 	I2 	I3 

Note: ■ ▲ ● indicate the level over the 1990s, 2000s and 2010s, respectively.

(2) Comparing the relative contributions of climate change and urbanization

Urbanization may have an indirect impact on the change in precipitation extremes. However, as global climate change is influenced by various human activities (IPCC, 2022), it is challenging to isolate the impacts of urbanization from those of climate change. In accordance with previous studies (e.g., Jones et al., 2015; Mondal et al., 2022; Zhou et al., 2019), this study made an assumption that the indirect impacts of human activities on climate change were not taken into account. The present study introduced the approach that isolated the impacts of urbanization and climate change by recalculating the urban flood hazard change when one factor was held constant (Jones et al., 2015; Mondal et al., 2022). The contribution rate of climate change or urbanization to urban flood hazard changes is calculated as follows:

$$Con = \frac{R_{t_2} - R_{t_1}}{R_{t_1}} \times 100\% \tag{8}$$

where *Con* indicates the contribution rate (%) of a given factor (climate change or urbanization) to urban flood hazard changes; R_{t_1} and R_{t_2} is the urban flood hazard calculated in the t_1 and t_2 periods, respectively. In calculating the contribution of climate change, we maintained constant land-use data and other inputs while altering only the climate data inputs. Specifically, the calculations for R_{t_1} and R_{t_2} were performed using unchanging land-use data and other inputs from the t_1 period, but with the climate data from their respective corresponding periods. Likewise, to assess the contribution of urbanization, we kept the climate data and other inputs stable, altering only the land-use data input from the t_1 period to the t_2 period.

The land-use type data in 1980, 1995, 2005, and 2015 were used to represent the land use over 1980–1989 (1980s), 1990–1999 (1990s), 2000–2009 (2000s), and 2010–2019 (2010s), respectively. Within the land use dataset, for the decade of 1980–1989, only data from the year 1980 is available. This is primarily due to no significant changes being found during this period. Additionally, as China's reform and opening-up policy commenced in 1978, previous studies often used data from around that year as a baseline for urbanization studies (e.g., Luo and Zhang, 2022; Tu et al., 2021). Given these cases, we used the 1980 data to depict the initial land-use patterns in China's major cities. The reason for using only one year in each decade is due to the methodology described above. Given that averaging land use types over a ten-year period is impractical, we chose to use the representative land use type from the midpoint year of each decade.

(3) Identifying the hotspot cities of urban flood hazard changes over the past decades

By conducting an analysis of the contribution rates of climate change and urbanization in each decade relative to the 1980s level, the temporal trend of their impacts could be determined. The comprehensive depiction of these impacts is presented in Fig. 2. Overall, these impacts can be classified into four types. Level I cities experienced increases in the impacts of both climate change and urbanization. Level II cities exhibited an increase in the climate change impact and a decrease in the urbanization impact. Conversely, Level III cities showed an increase in the urbanization impact and a decrease in the climate change impact. Finally, Level IV cities exhibited decreasing trends in the impacts of both factors. Accordingly, this study could assess the development patterns of urban flood hazards in China's major cities and identify the hotspot cities under the impacts of climate change and urbanization over the past decades.

3. Results

3.1. Changes in extreme precipitation and urban land area

As shown in Fig. 3a, from the 1980s–1990s, extreme precipitation increased in about 65% of the cities examined. These cities were mainly found in the south of Region I, the west of Region II, and most of Regions III and IV. In Regions VII and VIII, there was a slight increase (<5 mm) in most cities. These decreases were mainly found in the south of Region II and most of Region VI. During the 2000s, the south of Region I and the north of Region III exhibited decreases in the extreme precipitation relative to the baseline level (Fig. 3b). There were more cities with an increase in extreme precipitation in Region II. During the 2010s, extreme precipitation increased in approximately 70% of cities relative to the baseline level (Fig. 3c). Significant increases (>10 mm) were found in Regions III and IV. There were more cities with an increase in extreme precipitation in the south of Region VII. As shown in Fig. 3d, during the 1980–2010s, approximately 65% of cities exhibited an increase in extreme precipitation in the latest decade. These cities were mainly found in most of Regions I, III, VI, and VII. In particular, a trend of continuous (I2) increase during the past decades was found in the east of Region III, most of Region VI, and the south of Region VII. In many parts of Region II, precipitation extremes decreased over the latest decades. The majority of changes fell within 5%, while a smaller proportion exceeded 20%. The percentage of the increase in extreme precipitation was highest in the 2010s (Fig. S2).

As shown in Fig. 4a, from the 1980s–1990s, the ratio of urban land area increased in approximately 85% of cities across China. The cities with larger increases in the urban land area were mainly distributed in a small area of Region IV. There were some cities with a decrease in the urban land area scattered in some portions of Region I. During the 2000s, the ratio of urban land area increased relative to the baseline level in about 95% of cities (Fig. 4b). The increase in urban land area was more than 10% in some areas of Regions II, III, and IV. During the 2010s, there were more cities with larger increases in the urban land area relative to the baseline level (Fig. 4c). Significant increases were found in most of Region II and the east of Region III. As shown in Fig. 4d, during the 1980s–2010s, the urban land area continuously increased in approximately 90% of cities across China. During the 1990s and 2000s, the increase in the ratio of urban land area was generally less than 5%. During the 2010s, the proportion of cities with an increase of greater than 5% rose to about 40%. These cities were mainly distributed in Region II. The proportion of cities with a decrease in the ratio of urban land area declined greatly from the 1980s–2010s (Fig. S3).

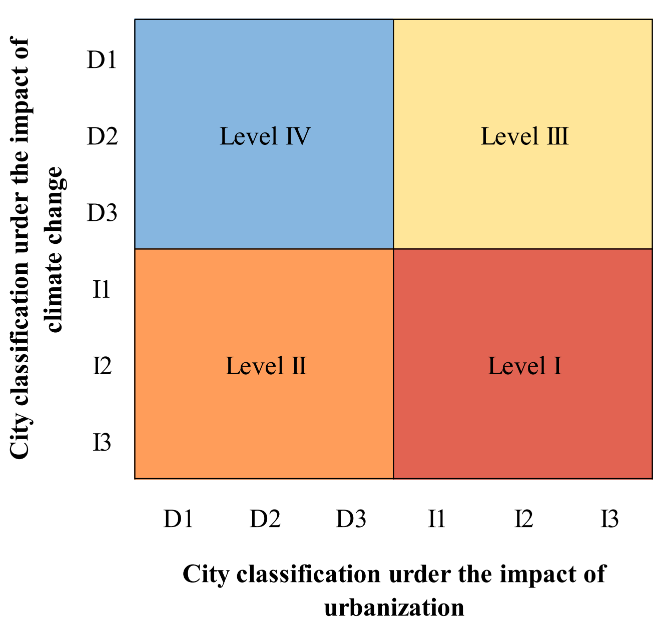

Fig. 2. Trend patterns under the impacts of climate change and urbanization.

3.2. Changes in urban flood hazard during 1980–2019

Changes in the urban flood hazard across China during the 1980s–2010s are presented in Fig. 5. Over the 1990s, the urban flood hazard increased in about 65% of cities. These cities were mainly found in the south of Region I, the east of Region II, and most of Regions III and IV (Fig. 5a). The increase was slight in Regions VII and VIII. The decrease was mainly found in most of Region VI and the south of Region VII. During the 2000s, the south of Region I and the north of Region III exhibited a decrease in urban flood hazard relative to the baseline level (Fig. 5b). There were more cities with an increase in the urban flood hazard in Region II. During the 2010s, the urban flood hazard increased in approximately 75% of cities relative to the baseline level (Fig. 5c). The cities with significant increases were mainly found in Region III. There were more cities with an increase in the urban flood hazard in the south of Region VII.

As shown in Fig. 5d, from the 1980s–2010s, approximately 70% of cities exhibited an increase in urban flood hazard in the latest decade. These cities were mainly found in Regions I, III, VI, and VII. In particular, in the east of Region III, most of Region VI, and the south of Region VII, a trend of continuous increase (I2 type) during the past decades was found. In the south of Region II, the urban flood hazard decreased over the latest decade. Fig. 6 presents the proportion of cities with different changes in urban flood hazard. The majority of changes fell within 5%, while a smaller proportion exceeded 15%. The percentage of cities with increased urban flood hazard levels was the highest in the 2010s.

3.3. Contributions of climate change and urbanization to urban flood hazard changes

The contributions of climate change and urbanization to urban flood hazard increases are shown in Fig. 7. In approximately 70% of cities across China, the contribution of climate change to the urban flood hazard increase was positive. Among these cities, the contribution of climate change to increased urban flood hazard was more than 50% in some cities located in Regions III and VII. The cities with negative contributions of climate change to increased urban flood hazard were mainly found in the south of Region II and most of Region VI. The contribution of urbanization to increased urban flood hazard was

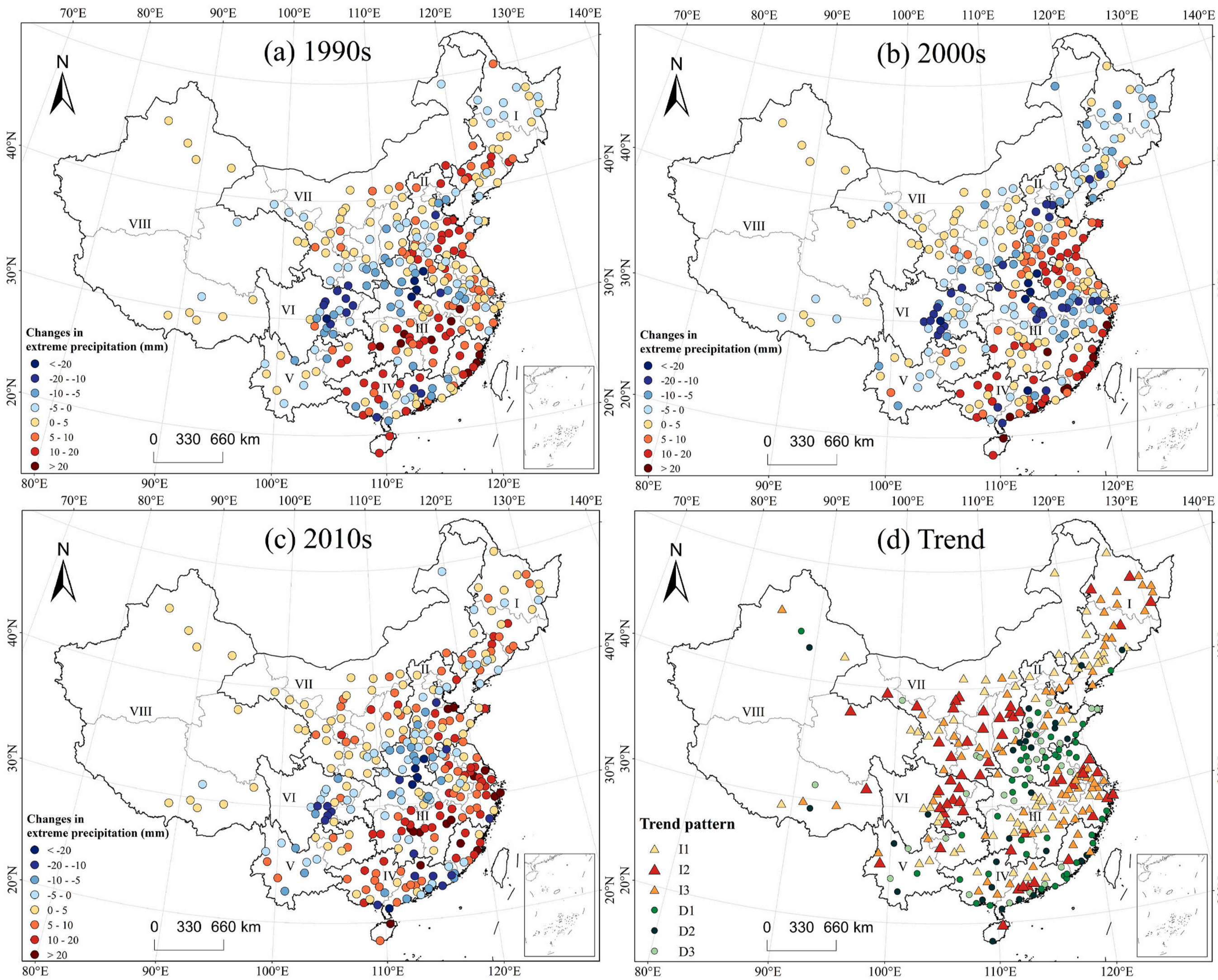

Fig. 3. Changes in extreme precipitation (mm) over the 1990s (a), 2000s (b), and 2010s (c) relative to that over the 1980s; temporal trend patterns of extreme precipitation from the 1980s–2010s (d).

positive in approximately 90% of cities across China. The majority of contribution rates fell within 25%. As shown in Fig. 8, urbanization typically contributes to an increase in urban flood hazards, while the contribution of climate change is not consistently in the same direction. In terms of absolute values, the impact of climate change far exceeded the impact of urbanization.

3.4. Identification of the hotspots of urban flood hazard changes over recent decades

As shown in Fig. 9, under the impact of climate change, the urban flood hazard increased consistently in some cities located in the east of Region III, most of Region VI, and the south of Region VII from the 1980s–2010s. In the latest decade, about 65% of cities exhibited an increase in urban flood hazard driven by climate change. These cities were mainly distributed in Regions I, III, IV, VI, and VII. The cities with a decrease in the urban flood hazard driven by climate change were mainly found in Region II and the south of Region IV. Under the impact of urbanization, the urban flood hazard increased continuously from the 1980s–2010s in about 68% of cities across China. These cities were mainly distributed in Regions II, III, IV, and V.

As shown in Fig. 10, half of the cities exhibited a Level I impact trend pattern, indicating that both the impacts of climate change and urbanization increased, particularly over the 2010s. These cities were mainly located in Regions I, III, IV, and VI. In most cities located in Region VII, the impact of climate change increased, whereas the impact of urbanization decreased (Level II type). About 30% of cities showed an increase in the impact of urbanization and a decrease in the impact of climate change (Level III type). These cities were mainly distributed in Region II. The 148 cities that exhibited the Level I impact trend pattern should receive more attention (Table S2). Specifically, 33 cities exhibited continuous increases in the impacts of both climate change and urbanization, namely, Lincang, Yunfu, Baoshan, Liuan, Liupanshui, Neijiang, Nantong, Hefei, Jilin, Taiyuan, Ningbo, Ankang, Guangyuan, Guangan, Guangzhou, Xinzhou, Yangzhou, Zhuzhou, Yongzhou, Haikou, Yancheng, Shizuishan, Mianyang, Zhaoqing, Zhoushan, Wuhu, Ziyang, Chongqing, Yinchuan, Zhenjiang, Yangquan, Jixi, and Qiqihar.

4. Discussion

4.1. Urban flood hazard changes under climate change and urbanization

In this research, we identified changes in precipitation extremes as the principal factor driving the evolution of urban flood hazards, corroborating the findings from previous studies (Hou et al., 2022; Sun et al., 2021; Wang et al., 2023). Over the past few decades, the observed

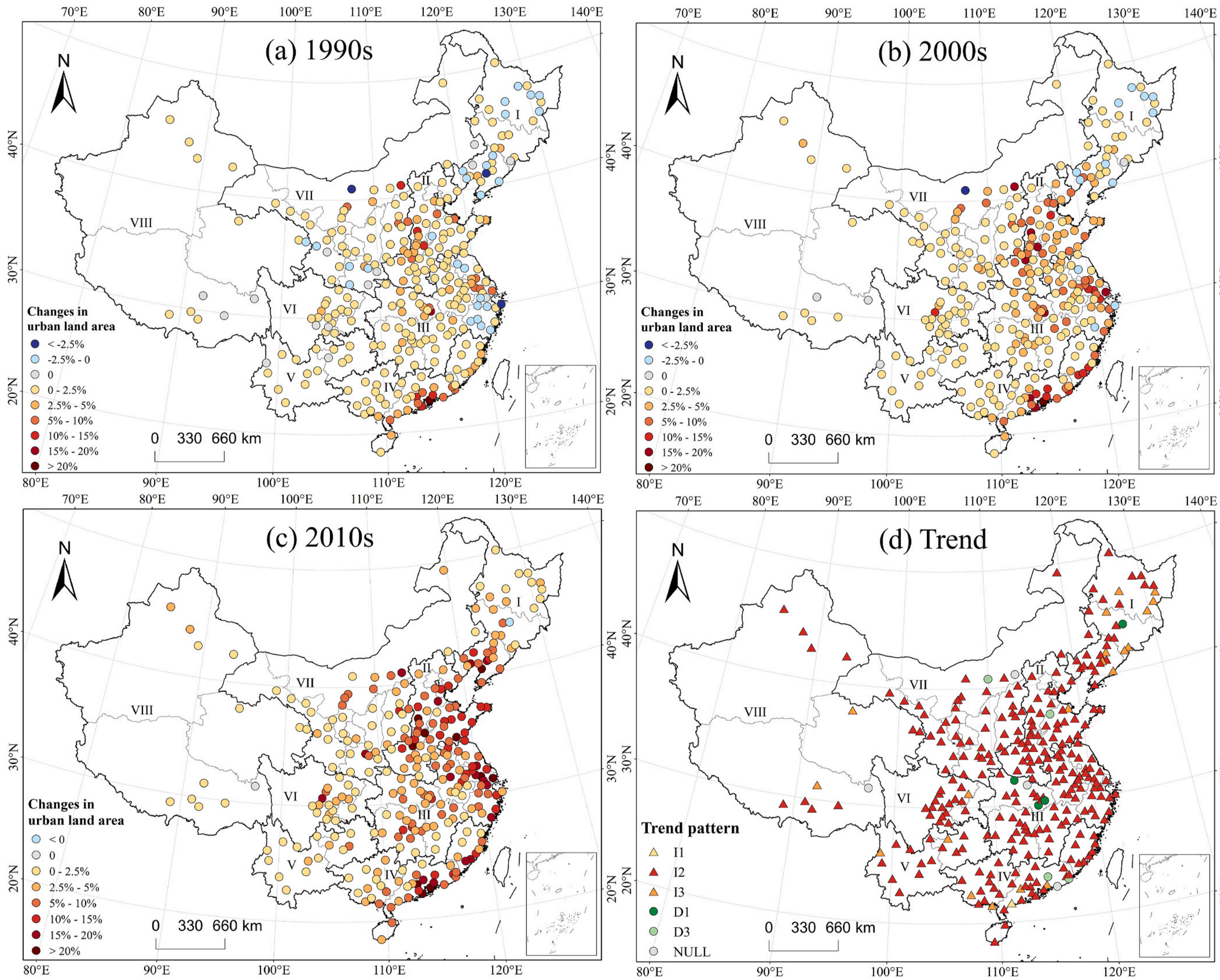

Fig. 4. Changes in the ratio of urban land area (%) over the 1990s (a), 2000s (b), and 2010s (c) relative to that over the 1980s; temporal trend patterns of the ratio of urban land area from the 1980s–2010s (d).

trend in urban flood hazards aligns closely with the changes in precipitation extremes documented in other researches (Shao et al., 2015; Zhao et al., 2019). For instance, in the Beijing-Tianjin-Tangshan area in northern Region II, Shao et al. (2015) reported a decreasing frequency of extreme precipitation events from 1950 to 2010. Zhao et al. (2019) observed a consistent decline in annual extreme precipitation days in the Yellow River Basin (YRB) located in eastern Region II from 1961 to 2002, with a modest downward trend, except in central YRB, from 2003 to 2016. These trends of urban flood hazard could also be detected in this study (Fig. 5). Furthermore, our study highlights the positive contribution of urbanization to the increase of urban flood hazards, a conclusion that finds support in the study of Luo and Zhang (2022). They demonstrated a significant decline in the urban flood regulation service capacity across most of the major cities from 1977 to 2018 due to land use/cover changes. This evidence underscores the substantial increase in urban flooding risk associated with urban land conversion, aligning with the period of rapid urbanization in China since the mid-1980s extensive economic reforms.

4.2. Indications for adaptation strategies

Mitigating climate change is not an easy task, necessitating extensive global-scale efforts (IPCC, 2022). Substantial management measures should be explored in the study on a global scale. In regional-scale studies, urban flood risk management typically involves measures for managing urban development and adapting to climate change (e.g., Sun et al., 2021; Zhou et al., 2018). In the cities of Regions I, III, IV, and VI, the impacts of both climate change and urbanization increased continuously during recent decades. These cities should dedicate more attention to future urban flood risks. The magnitudes of precipitation extremes have been projected to show upward variations in most areas across China under future climate change (Tian et al., 2021; Xu et al., 2022). Given that changes in precipitation serve as the major driver of urban flood hazard changes, global-scale climate change mitigation should achieve obvious effects. Anthropogenic drivers of climate change, including greenhouse gases, aerosols, and land use, should be developed optimally during the future period (O'Neill et al., 2016). The 18th National Congress of the Communist Party of China has put forward a new type of urbanization development strategy that stresses the full integration of improvements in ecology quality into urban development (Yu, 2021). However, in some first-tier cities, the impacts of rapid urbanization should continue to receive attention. For example, the urbanization process still serves as the major factor in increasing the flood risk of the Yangtze River Economic Belt (YREB) (Peng and Li, 2021). In these cities, local adaptation measures can be implemented to cope with the increase in urban flood hazard caused by future climate

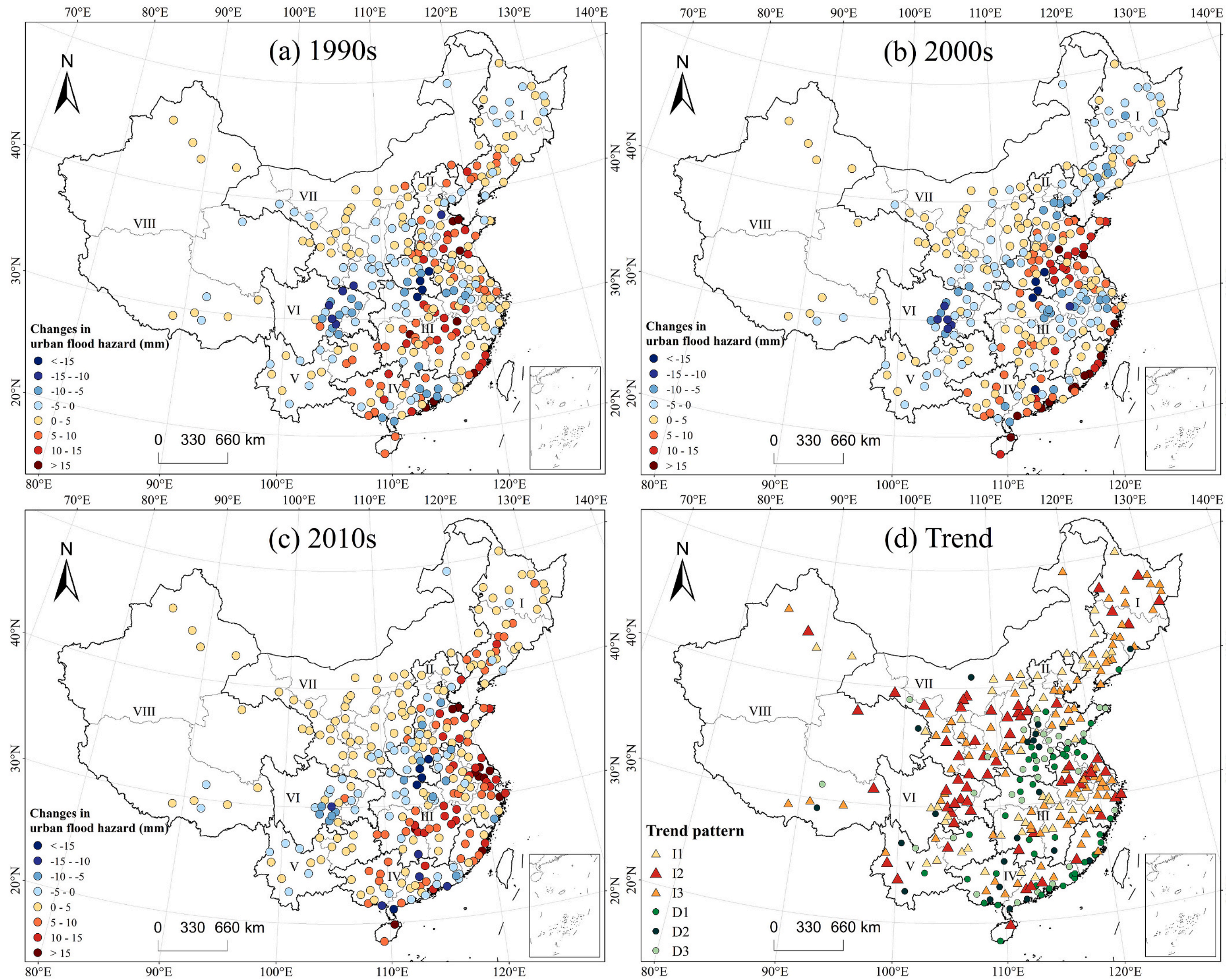

Fig. 5. Changes in urban flood hazard (mm) over the 1990s (a), 2000s (b), and 2010s (c) relative to that over the 1980s; temporal trend patterns of urban flood hazard from the 1980s–2010s (d).

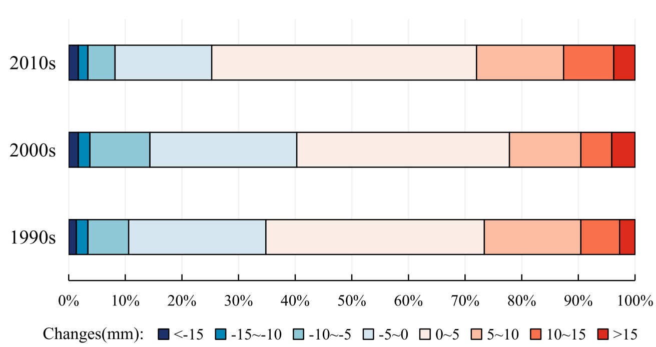

Fig. 6. Proportions of cities with different changes in urban flood hazard (mm) over each decade relative to the level over the 1980s.

change. Measures including pipe enlargement and low-impact development (LID) have been demonstrated to be effective in some cities (e.g., Hohhot City and central Shanghai) (Sun et al., 2021; Zhou et al., 2018). Specifically, LID measures generally include the use of green roofs, infiltration trenches and permeable pavements (Abduljaleel and Demissie, 2021; Azari and Tabesh, 2022; Ghodsi et al., 2020; Pour et al., 2020). As indicated by previous studies (Kourtis and Tsihrintzis, 2021; Wang et al., 2023), surface retention capacity enhancements and pipe enlargement measures would substantially reduce the pressure of urban drainage system in the cities of eastern China.

4.3. Limitations and future study

The results of this study are more suited to capturing the temporal changes in urban flood hazard than being interpreted as the absolute level in a given year/decade. At the grid scale, some factors (e.g., micro-climate and micro-terrain) were not fully considered, which might affect the calculation of urban flood hazards and lead to some uncertainties in the results. Limitations exist in accurately isolating the impacts of urbanization from those of climate change. In practical applications, the changes in the hydrological cycle induced by urbanization should be considered as well. The existing literature suggests multiple methods for defining extreme precipitation; in this analysis we work with only one (P99). It may be useful to consider alternative and/or geographically specific definitions of extreme precipitation, such as the maximum precipitation or humidex over a specific number of consecutive days, to better understand changes in exposure to climate extremes.

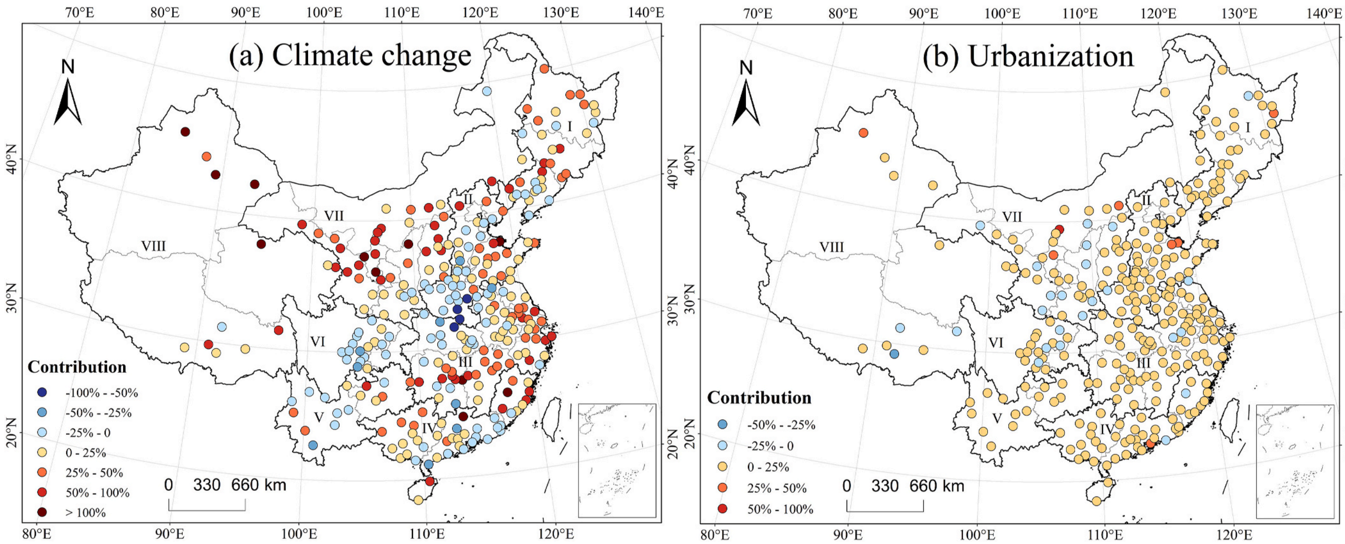

Fig. 7. Contributions of climate change (a) and urbanization (b) to urban flood hazard increases from the 1980s–2010s.

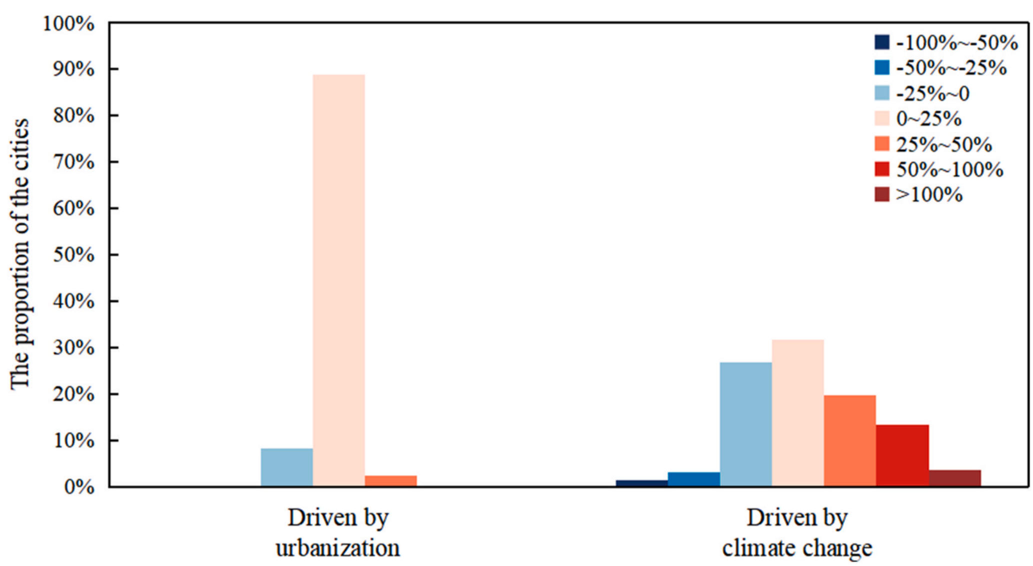

Fig. 8. Proportions of cities with different contributions of climate change and urbanization to the urban flood hazard increase from the 1980s–2010s.

5. Conclusions

This study used surface runoff calculations as the urban flood hazard and assessed the changes in precipitation extremes, urban land area, and urban flood hazard in China's 293 major cities from the 1980s–2010s. Based on the decomposition analysis, this study quantified the relative contributions of climate change and urbanization to urban flood hazard changes and identified the hotspot cities with consecutive increases under the impacts of both factors. The main conclusions are as follows.

(1) From the 1980s–2010s, cities mainly concentrated in the east of Region III, most of Region VI, and the south of Region VII exhibited consistent increases in precipitation extremes. In the latest decade, more than half of the cities investigated showed an increase in extreme precipitation. Over these three decades, the urban land area increased continuously in most of China's major cities. Urban flood hazard has increased consistently mainly in the cities of Regions III and VI.
(2) In terms of the absolute rate, the contribution of climate change far outweighed that of urbanization. The contribution of urbanization to increased urban flood hazard was positive in more than 90% of cities. However, the contribution directions of climate change to increased urban flood hazard were quite different across China. In approximately 70% of cities, the contribution of climate change to urban flood hazard increases was positive.
(3) Cities that showed an increase in the impact of urbanization but a decrease in the impact of climate change were mainly distributed in Region II. The impacts of climate change and urbanization increased over the latest decade in half of the cities, which were mainly distributed in northeastern and southeastern China. Specifically, 33 cities (identified as the hotspots) exhibited consecutive increases under the impacts of both climate change and urbanization, which should be tracked in the future.

Limitations exist in accurately isolating the impacts of urbanization from those of climate change. In practical applications, the changes in the hydrological cycle induced by urbanization should be considered as well. To better understand changes in climate extremes, it may be useful to consider alternative and/or geographically specific definitions of

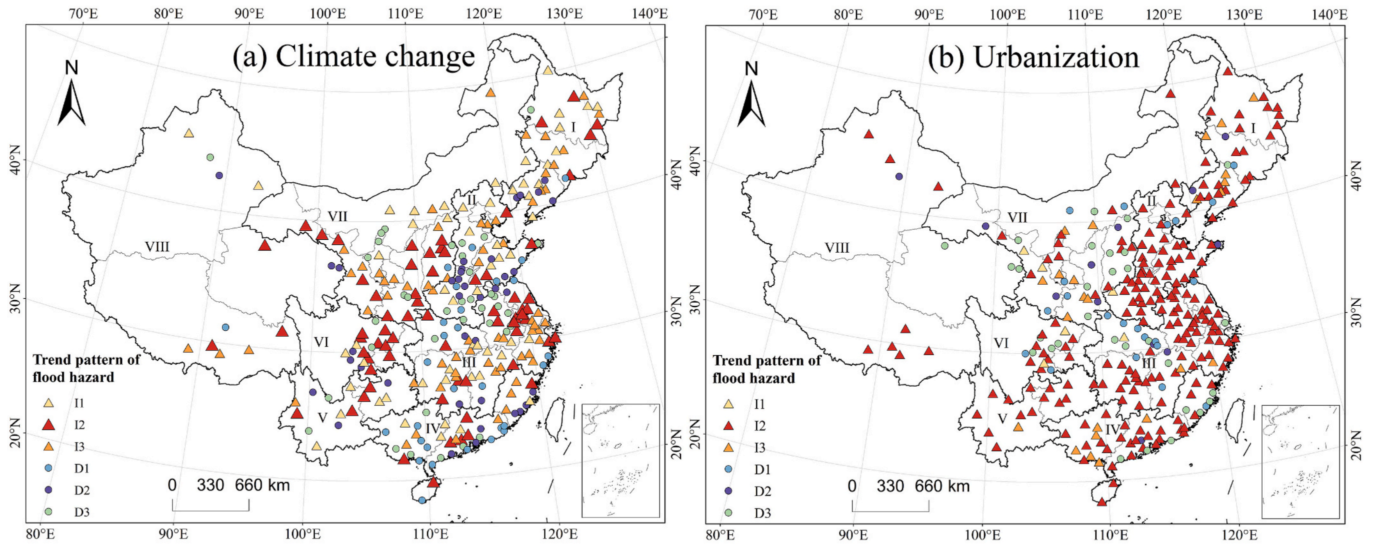

Fig. 9. Trend patterns of urban flood hazard changes driven by climate change (a) and urbanization (b).

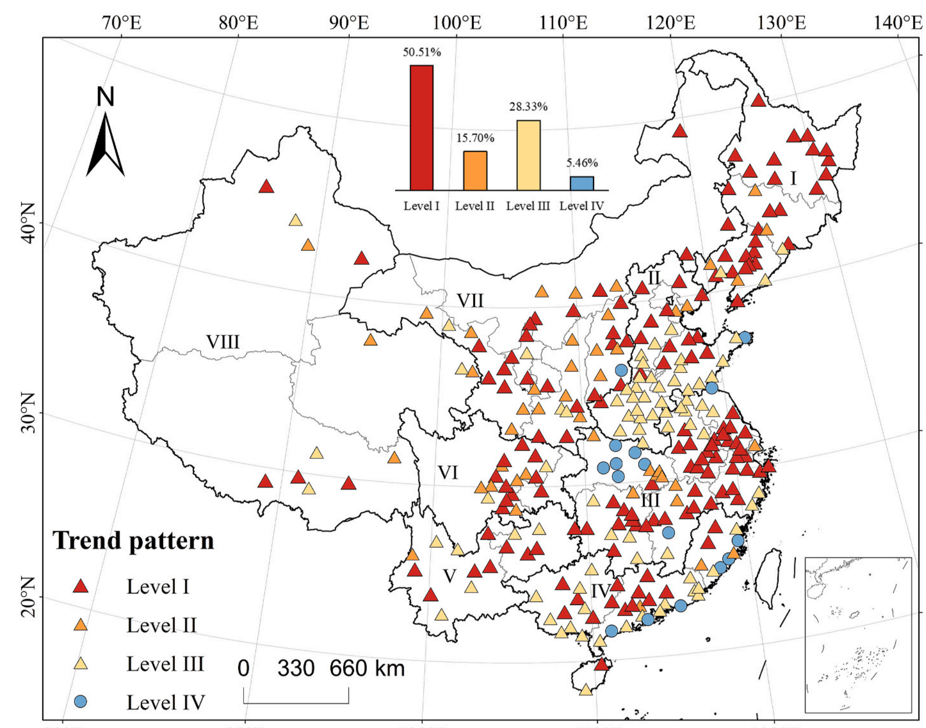

Fig. 10. Trend patterns of the impacts of climate change and urbanization in China's major cities.

extreme precipitation, such as maximum precipitation or humidex over a specific number of consecutive days. Despite these limitations, this approach is expected to be effective in large-scale applications and areas with limited data availability. And the findings of this study do provide the first quantitative basis for examining the impacts of urbanization and climate change across China's major cities using a consistent framework, and potentially provide valuable insights for the development of national management strategies in the face of ongoing environmental changes.

CRediT authorship contribution statement

Ziyi Tang: Writing – original draft, Software, Methodology, Investigation, Data curation. **Pin Wang:** Methodology, Formal analysis, Writing – review & editing. **Yao Li:** Validation, Software, Methodology, Formal analysis. **Yue Sheng:** Writing – review & editing. **Ben Wang:** Writing – review & editing, Visualization. **Nataliia Popovych:** Writing – review & editing. **Tangao Hu:** Writing – review & editing, Validation.

Declaration of competing interest

The authors declare that they have no known competing financial interests or personal relationships that could have appeared to influence the work reported in this paper.

Data availability

Data will be made available on request.

Acknowledgments

This work was supported by the National Natural Science Foundation of China (Grant No. 41807506), Zhejiang Provincial Natural Science Foundation of China (Grant No. LQ18D010007).

Appendix A. Supplementary data

Supplementary data to this article can be found online at https://doi.org/10.1016/j.jenvman.2024.120113.

References

Abduljaleel, Y., Demissie, Y., 2021. Evaluation and optimization of low impact development designs for sustainable stormwater management in a changing climate. Water 13 (20), 2889.

Azari, B., Tabesh, M., 2022. Urban storm water drainage system optimization using a sustainability index and LID/BMPs. Sustain. Cities Soc. 76, 103500.

Beshir, A., Song, J., 2021. Urbanization and its impact on flood hazard: the case of Addis Ababa, Ethiopia. Nat. Hazards 109 (1), 1167–1190.

Blöschl, G., Hall, J., Viglione, A., Perdigão, R.A., Parajka, J., Merz, B., et al., 2019. Changing climate both increases and decreases European river floods. Nature 573 (7772), 108–111.

Cao, S., Zhang, Z., 2022. Towards a "County-Free era"? - summary and reflection on the practice of converting counties to districts in contemporary China. Open 4, 62–77.

Chen, X., Zhang, H., Chen, W., Huang, G., 2021. Urbanization and climate change impacts on future flood risk in the Pearl River Delta under shared socioeconomic pathways. Sci. Total Environ. 762, 143144.

Disaster Investigation Team of State Council, 2022. Investigation Report on July 20, 2021 Torrential Rain Disaster in Zhengzhou, Henan Province, China.

Ghodsi, S., Zahmatkesh, Z., Goharian, E., Kerachian, R., Zhu, Z., 2020. Optimal design of low impact development practices in response to climate change. J. Hydrol. 580, 124266.

Gou, J.J., Miao, C.Y., Duan, Q.Y., Tang, Q.H., Di, Z.H., Liao, W.H., Wu, J.W., Zhou, R., 2020. Sensitivity analysis-based automatic parameter calibration of the VIC model for streamflow simulations over China. Water Resour. Res. 56, 1–19.

Gou, J.J., Miao, C.Y., Samaniego, L., Xiao, M., Wu, J.W., Guo, X.Y., 2021. CNRD v1.0: a high-quality natural runoff dataset for hydrological and climate studies in China. Bull. Am. Meteorol. Soc. 102 (5), E929–E947.

Hou, J., Zhang, Y., Xia, J., Wang, Y., Zhang, S., Pan, X., Yang, M., Leng, G., Dou, M., 2022. Simulation and assessment of projected climate change impacts on urban flood events: insights from flooding characteristic metrics. J. Geophys. Res. Atmos. 127 (3), e2021JD035360.

Hu, S., Fan, Y., Zhang, T., 2020. Assessing the effect of land use change on surface runoff in a rapidly urbanized city: a case study of the central area of Beijing. Land 9 (1), 17.

Huang, M.B., Gallichand, J., Wang, Z.L., Goulet, M., 2006. A modification to the Soil Conservation Service curve number method for steep slopes in the Loess Plateau of China. Hydrol. Process. 20 (3), 579–589.

IPCC (Intergovernmental Panel on Climate Change), 2022. In: Shukla, P.R., Skea, J., Slade, R., Al Khourdajie, A., van Diemen, R., McCollum, D., Pathak, M., Some, S., Vyas, P., Fradera, R., Belkacemi, M., Hasija, A., Lisboa, G., Luz, S., Malley, J. (Eds.), Climate Change 2022: Mitigation of Climate Change. Contribution of Working Group III to the Sixth Assessment Report of the Intergovernmental Panel on Climate Change. Cambridge University Press, Cambridge, UK and New York, NY, USA.

Jiang, R., Lu, H., Yang, K., Chen, D., Zhou, J., Yamazaki, D., Pan, M., Li, W., Xu, N., Yang, Y., Guan, D., Tian, F., 2023. Substantial increase in future fluvial flood risk projected in China's major urban agglomerations. Communications Earth & Environment 4 (1), 389.

Jones, B., O'Neill, B.C., McDaniel, L., McGinnis, S., Mearns, L.O., Tebaldi, C., 2015. Future population exposure to US heat extremes. Nat. Clim. Change 5 (7), 652–655.

Kourtis, I., Tsihrintzis, V., 2021. Adaptation of urban drainage networks to climate change: a review. Sci. Total Environ. 771, 145431.

Li, C., Liu, M., Hu, Y., Wang, H., Zhou, R., Wu, W., Wang, Y., 2022. Spatial distribution patterns and potential exposure risks of urban floods in Chinese megacities. J. Hydrol. 610, 127838.

Li, C., Liu, M., Hu, Y., Shi, T., Qu, X., Walter, M., 2018. Effects of urbanization on direct runoff characteristics in urban functional zones. Sci. Total Environ. 643, 301–311.

Li, Y., Zhao, S., 2022. Study on flood loss and disaster risk in China from 2001 to 2020. Progress in climate change research 18 (2), 154–165.

Liang, C., Li, D., Yuan, Z., Liao, Y., Nie, X., Huang, B., Wu, X., Xie, Z., 2019. Assessing urban flood and drought risks under climate change, China. Hydrol. Process. 33 (9), 1349–1361.

Liu, Y., Huang, X., Yang, H., 2022. An integrated approach to investigate the coupling coordination between urbanization and flood disasters in China. J. Clean. Prod. 375, 134191.

Liu, J., Kuang, W., Zhang, Z., Xu, X., Qin, Y., Ning, J., Zhou, W., Zhang, S., Li, R., Yan, C., Wu, S., Shi, X., Jiang, N., Yu, D., Pan, X., Chi, W., 2014. Spatiotemporal characteristics, patterns, and causes of land-use changes in China since the late 1980s. J. Geogr. Sci. 24 (2), 195–210.

Luo, K., Zhang, X., 2022. Increasing urban flood risk in China over recent 40 years induced by LUCC. Landsc. Urban Plann. 219, 104317.

Lyu, H.M., Zhou, W.H., Shen, S.L., Zhou, A.N., 2020. Inundation risk assessment of metro system using AHP and TFN-AHP in Shenzhen. Sustain. Cities Soc. 56, 102103.

Mahmoud, S.H., Gan, T.Y., 2018. Urbanization and climate change implications in flood risk management: developing an efficient decision support system for flood susceptibility mapping. Sci. Total Environ. 636, 152–167.

Miao, C.Y., Gou, J.J., Fu, B.J., Tang, Q.H., Duan, Q.Y., Chen, Z.S., Lei, H.M., Chen, J., Guo, J.L., Borthwick, A.G.L., Ding, W.F., Duan, X.W., Li, Y.G., Kong, D.X., Guo, X.Y., Wu, J.W., 2022. High-quality reconstruction of China's natural streamflow. Sci. Bull. 67 (5), 547–556.

Mishra, S.K., Singh, V., 2003. Soil Conservation Service Curve Number (SCS-CN) Methodology. Kluwer Academic Publishers, Dordrecht, The Netherlands.

Mondal, S.K., Wang, Y., Zhai, J., Su, B., Jiang, S., Huang, J., Jing, C., Lin, Q., Zhou, J., Gao, M., 2022. Projected urban exposure to extreme precipitation over South Asia. Sci. Total Environ. 822, 153664.

Neitsch, S.L., Arnold, J.G., Kiniry, J.R., Williams, J.R., 2011. Soil and Water Assessment Tool Theoretical Documentation Version 2009. Texas Water Resources Institute.

O'Neill, B.C., Tebaldi, C., Van Vuuren, D.P., Eyring, V., Friedlingstein, P., Hurtt, G., Knutti, R., Kriegler, E., Lamarque, J., Lowe, J., 2016. The scenario model intercomparison project (ScenarioMIP) for CMIP6. Geosci. Model Dev. (GMD) 9 (9), 3461–3482, 2016.

Pang, S., Wang, X., Melching, C.S., Feger, K.H., 2020. Development and testing of a modified SWAT model based on slope condition and precipitation intensity. J. Hydrol. 588, 125098.

Peng, X., Zhou, Y., Fu, X., Xu, J., 2022. Study on the spatial-temporal pattern and evolution of surface urban heat island in 180 shrinking cities in China. Sustain. Cities Soc. 84, 104018.

Peng, S., Ding, Y., Liu, W., Li, Z., 2019. 1km monthly temperature and precipitation dataset for China from 1901 to 2017. Earth System Science Data 11 (4), 1931–1946.

Peng, L., Li, Z., 2021. Ensemble flood risk assessment in the Yangtze River Economic Belt under CMIP6 SSP-rcp scenarios. Sustainability 13 (21), 12097.

Pour, S., Abd Wahab, A., Shahid, S., Asaduzzaman, M., Dewan, A., 2020. Low impact development techniques to mitigate the impacts of climate-change-induced urban floods: current trends, issues and challenges. Sustain. Cities Soc. 62, 102373.

Rentschler, J., Avner, P., Marconcini, M., Su, R., Strano, E., Vousdoukas, M., Hallegatte, S., 2023. Global evidence of rapid urban growth in flood zones since 1985. Nature 622 (7981), 87–92.

Shao, Y., Wu, J., Ye, J., Liu, Y., 2015. Frequency analysis and its spatiotemporal characteristics of precipitation extreme events in China during 1951-2010. Theor. Appl. Climatol. 121 (3), 775–787.

Shi, J., Cui, L., Tian, Z., 2020. Spatial and temporal distribution and trend in flood and drought disasters in East China. Environ. Res. 185, 109406.

Sun, X., Li, R., Shan, X., Xu, H., Wang, J., 2021. Assessment of climate change impacts and urban flood management schemes in central Shanghai. Int. J. Disaster Risk Reduc. 65, 102563.

Tellman, B., Sullivan, J., Kuhn, C., Kettner, A., Doyle, C., Brakenridge, G., et al., 2021. Satellite imaging reveals increased proportion of population exposed to floods. Nature 596 (7870), 80–86.

Tian, J., Zhang, Z., Ahmed, Z., Zhang, L., Su, B., Tao, H., Jiang, T., 2021. Projections of precipitation over China based on CMIP6 models. Stoch. Environ. Res. Risk Assess. 35 (4), 831–848.

Tu, Y., Chen, B., Yu, L., Xin, Q., Gong, P., Xu, B., 2021. How does urban expansion interact with cropland loss? A comparison of 14 Chinese cities from 1980 to 2015. Landsc. Ecol. 36 (1), 243–263.

U. S. Soil Conservation Service, 1972. National Engineering Handbook, Section 4: Hydrology. U. S: Department of Agriculture.

Verma, R.K., Verma, S., Mishra, S.K., Pandey, A., 2021. SCS-CN-based improved models for direct surface runoff estimation from large rainfall events. Water Resour. Manag. 35 (7), 2149–2175.

Wang, C., Jiang, Q., Shao, Y., Sun, S., Xiao, L., Guo, J., 2019. Ecological environment assessment based on land use simulation: a case study in the Heihe River Basin. Sci. Total Environ. 697, 133928.

Wang, P., Li, Y., Fan, J., Kong, F., Zhang, D., Hu, T., 2023. Future changes in urban drainage pressure caused by precipitation extremes in 285 cities across China based on CMIP6 models. Sustain. Cities Soc. 91, 104404.

Xu, H., Chen, H., Wang, H., 2022. Future changes in precipitation extremes across China based on CMIP6 models. Int. J. Climatol. 42 (1), 635–651.

Yang, W., Zhang, J., Krebs, P., 2023. Investigating flood exposure induced socioeconomic risk and mitigation strategy under climate change and urbanization at a city scale. J. Clean. Prod. 387, 135929.

Yin, J., He, F., Xiong, Y., Qiu, G., 2017. Effects of land use/land cover and climate changes on surface runoff in a semi-humid and semi-arid transition zone in northwest China. Hydrol. Earth Syst. Sci. 21, 183–196.

Yu, B., 2021. Ecological effects of new-type urbanization in China. Renew. Sustain. Energy Rev. 135, 110239.

Zhang, D., Wang, X., Qu, L., Li, S., Lin, Y., Yao, R., Zhou, X., Li, J., 2020. Land use/cover predictions incorporating ecological security for the Yangtze River Delta region, China. Ecol. Indicat. 119, 106841.

Zhang, K., Li, C., 2021. The course, features and prospects of administrative division adjustment in China's 70 Years since the founding of new China. J. Soc. Sci. 1, 118–128.

Zhao, Y., Xu, X., Huang, W., Wang, Y., Xu, Y., Chen, H., Kang, Z., 2019. Trends in observed mean and extreme precipitation within the Yellow River Basin, China. Theor. Appl. Climatol. 136 (3), 1387–1396.
Zhou, Q., Leng, G., Huang, M., 2018. Impacts of future climate change on urban flood volumes in Hohhot in northern China: benefits of climate change mitigation and adaptations. Hydrol. Earth Syst. Sci. 22 (1), 305–316.
Zhou, Q., Leng, G., Su, J., Ren, Y., 2019. Comparison of urbanization and climate change impacts on urban flood volumes: importance of urban planning and drainage adaptation. Sci. Total Environ. 658, 24–33.